BB

PREPRINT

TASCC-P-95-5

tascc

Reaction Mechanisms of the Most Violent $^{24}Mg + ^{12}C$ Collisions at 25A and 35A MeV

Y. Larochelle[a], G.C. Ball[b], L. Beaulieu[a], B. Djerroud[a 1], D. Dore[a 2], A. Galindo-Uribarri[b], P. Gendron[a], E. Hagberg[b], D. Horn[b], E. Jalbert[a], R. Laforest[a 3], J. Pouliot[a 4], R. Roy[a], M. Samri[a] and C. St-Pierre[a]

[a] *Laboratoire de physique nucléaire, Département de physique, Université Laval, Québec, Canada G1K 7P4*

[b] *AECL, Chalk River Laboratories, Ontario , Canada K0J 1J0*

[1] *Present address: NSRL, University of Rochester, New York, USA*

[2] *Present address: IPN de Lyon, Villeurbanne, France*

[3] *Present address: LPC de Caen, Caen, France*

[4] *Present address: Hôtel-Dieu de Québec, Département de Radio-Oncologie, Québec, Canada*

To be published in the Proceedings of the Winter Workshop on Nuclear Dynamics, Key West, Florida, 1995 February 11-17

NOTICE

Physical and Environmental Sciences
Chalk River Laboratories
Chalk River, ON K0J 1J0 Canada

1995 February

Reaction Mechanisms of the Most Violent ^{24}Mg + ^{12}C Collisions at 25A and 35A MeV

Y. LAROCHELLE[a], G.C. BALL[b], L. BEAULIEU[a], B. DJERROUD[a 1], D. DORE[a 2], A. GALINDO-URIBARRI[b], P. GENDRON[a], E. HAGBERG[b], D. HORN[b], E. JALBERT[a], R. LAFOREST[a 3], J. POULIOT[a 4], R. ROY[a], M. SAMRI[a] and C. ST-PIERRE[a]

[a] *Laboratoire de physique nucléaire, Département de physique, Université Laval, Québec, Canada G1K 7P4*

[b] *AECL, Chalk River Laboratories, Ontario, Canada K0J 1J0*

ABSTRACT

A study of reaction mechanisms in central ^{24}Mg+^{12}C collisions at 25A and 35A MeV has been carried out. Global variables, such as anisotropy ratios and source-velocity ratios, computed for those events in which the total charge of the system has been detected, are compared to simulations based on statistical fragmentation codes. For violent events, a binary mechanism appears to be competing with compound nucleus formation.

1. Introduction

Central collisions between heavy ions at intermediate energies (*i.e.* between 10 and 100 MeV/nucleon), are known to result in multifragmentation [1,2] and other interesting phenomena. In an extrapolation from well-understood processes at lower energy, complete and, more likely, incomplete fusion accompanied by pre-equilibrum emission of light particles (for examples, see refs. [3,4,5,6]) have been proposed as the mechanisms responsible for formation of highly excited nuclear systems, which subsequently decay to the observed final states. Recently, however, a binary nature has been observed in collisions involving a high level of dissipation with the two excited partners retaining most of the kinematic characteristics of the projectile and the target[7,8]. The present paper reports an analysis of the most central collisions for a light system of 36 nucleons. Since a determination of the source properties for these events is essential, detection of the entire system is a prerequisite for a proper event-shape analysis. Our analysis is limited to collisions in which the total charge

[1]Present address: NSRL, University of Rochester, New York, USA
[2]Present address: IPN de Lyon, Villeurbanne, France
[3]Present address: LPC de Caen, Caen, France
[4]Present address: Hôtel-Dieu de Québec, Département de Radio-Oncologie, Québec, Canada

of the system (projectile+target) has been detected in an array of charged-particle counters. We compare the distributions of the reaction products in velocity space with the distributions predicted by two excitation scenarios representing opposite, limiting cases, namely complete fusion and dissipative binary collisions. A general trend, favouring a competition between compound nucleus formation and a dissipative binary mechanism is observed for violent channels.

2. Experimental Set-Up

The experiment was performed at the TASCC facility of Chalk River Laboratories (CRL), with beams of ^{24}Mg ions at 25A and 35A MeV, incident on a 2.4 mg/cm^2 C target. Reverse kinematics focussed reaction products into the 80-detector CRL-Laval Array. The array is comprised of three rings of 16 plastic phoswich scintillation detectors each, covering angles from 6^o to 24^o (sensitive to particles with Z=1 to Z=12) and two rings of 16 CsI(Tl) scintillators each, covering angles from 24^o to 46^o (sensitive to particles with Z=1 or Z=2). Each phoswich detector consists of a thick, slow-plastic E-detector and a 0.7 mm ΔE layer of fast plastic scintillator, heat-pressed to the front of the E detector [9]. Energy calibration data were obtained from secondary beams of Z=1 through 11, produced at the exit of the cyclotron, and ^{24}Mg ions elastically scattered from ^{197}Au targets. The phoswich detectors were calibrated according to the relation given in Ref. [10] and the CsI(Tl) detectors by the energy-light relation from Ref. [11]. The intrinsic energy resolution of the detectors was better than 5% and the precision of the energy-light relation was close to 5% for both types of detectors. The energy threshold varied from 7.5 to 19.6 MeV/nucleon for Z=1 to 12 for the phoswich detectors and was approximately 2 MeV/nucleon for Z=1 and 2 in the CsI(Tl) detectors. Isotopic identification for charge Z=1 was possible in the CsI(Tl) detectors in the 25A MeV experiment. For the other particles the assumed mass was that of the most abundant isotope.

The reconstructed velocity of the center of mass (CM) for the complete events provides a good test of whether pileup has been successfully excluded. Fig. 1 shows such a reconstruction for events with total detected charge ΣZ=18 and ΣZ=12, at 25A and 35A MeV, along with the calculated CM and beam velocity for both energies. Velocity reconstruction for detected events with ΣZ=12 demonstrates the bias that incomplete events would make on the analysis. As indicated by the vertical lines in the figure, complete events lying in the tails toward lower or higher velocities were excluded from the analysis. For exit channels with less ambiguity in the isotopic identification of the reaction products, further improvements in the reconstructed CM velocity may be achieved, as seen in Fig 8. of Ref. [11]. This fact is exploited in our analysis of the 9-He exit channel.

3. Data Analysis and Simulations

The experimental events in which the total system charge was detected (ΣZ=18) had charged-particle multiplicities between 5 and 12, and represented a wide variety

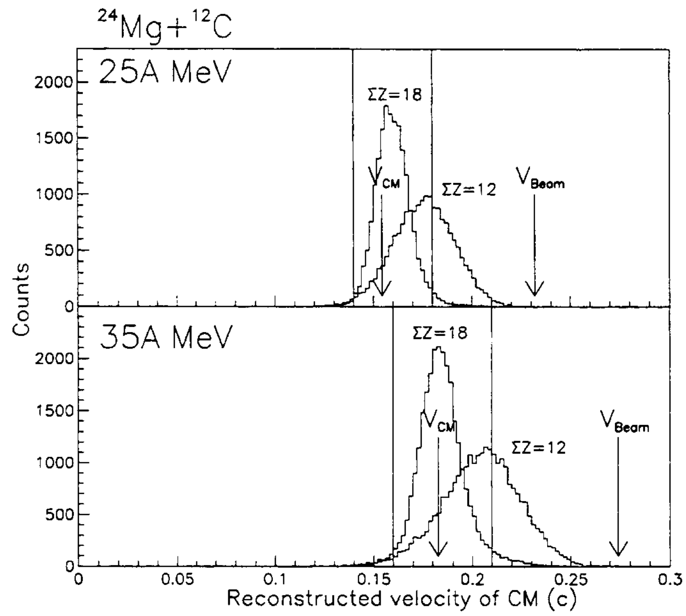

Fig. 1: Reconstructed center-of-mass velocity for exit channels with ΣZ=12 and ΣZ=18 from the ^{24}Mg+^{12}C reaction at 25A MeV (top) and 35A MeV (bottom). The arrows indicate beam velocity and CM velocity for the complete system of target plus projectile. Vertical lines show the ΣZ=18 events selected for further analysis.

of exit channels. Of the observed events, 63% consisted of one intermediate-mass fragment (IMF) of element number 3 to 11 along with hydrogen and helium ions, 28% had two or three IMFs plus light ions, and the remaining 9% were completely disassembled into light ions. The completely detected events represent an absolute cross-section of 8 mb at 25A MeV and 20 mb at 35A MeV, which is a small percentage of the total reaction cross-section, estimated at about 1600 mb in this energy range, following the prescription from Ref. [12]. The cross-section increase between 25A MeV and 35A MeV may be due to the increased detector acceptance for higher velocities.

A mid-rapidity charge parameter (Z_{mr}) [13] was used to evaluate the centrality of the events. At 25A MeV, 76% of the events had Z_{mr} greater than 15 and at 35A MeV the corresponding fraction was 62% , indicating the violent nature of the majority of the (ΣZ=18) events. Another way to probe the violence of a collision is to extract the ratio between the total transverse energy of a given event and the total energy in CM frame of the reaction for each beam energy. For completely detected events that ratio averaged 0.30 at 25A MeV and 0.27 at 35A MeV.

Possible reaction mechanisms for these violent events include dissipative binary collisions, as well as complete and incomplete fusion. Incomplete fusion reactions are largely eliminated in our analysis by the ΣZ=18 requirement. It has been shown [3,14] that when incomplete fusion reactions are viewed in reverse kinematics, the pre-equilibrum emission of target-like spectators is not forward-peaked in the laboratory frame. Since the probability is very low that all pre-equilibrium, target-like charged particles are emitted forward of 46^o and above detector threshold, we would not detect incomplete fusion reactions as complete events. Similarly, pre-equilibrum emission of

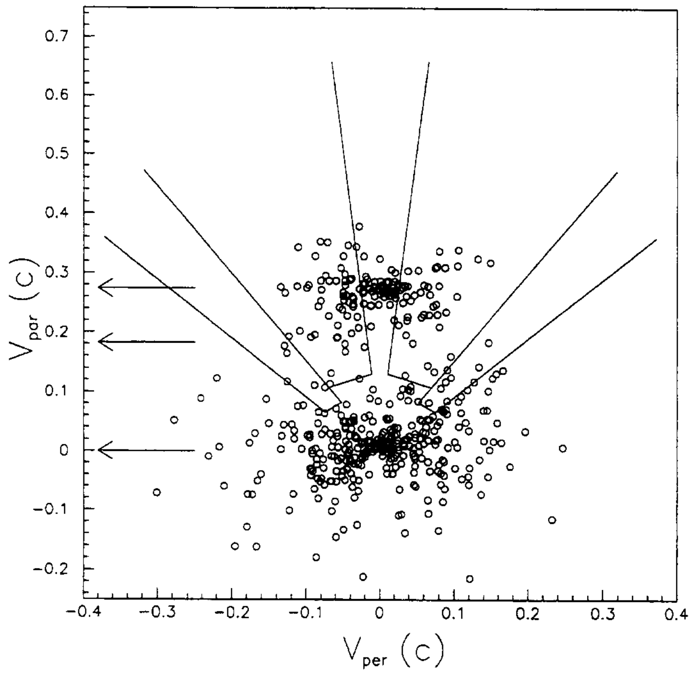

Fig. 2: Parallel versus perpendicular velocity plot of pre-equilibrum proton emission in an incomplete fusion scenario of $^{24}Mg + ^{12}C$ at $35A$ MeV simulated with the code GENEVE. Lines represent the geometric and energetic thresholds of the array of detectors for protons. Arrows show projectile (0.27c), CM (0.18c) and target (0.0c) velocities.

projectile-like spectators, though rare in reverse kinematics reactions, would be very forward-peaked, and mostly lost in the beam-exit port of the array. Simulations of incomplete fusion reactions were done with the code GENEVE [15] for the system at $35A$ MeV. Fig. 2 shows the parallel versus perpendicular velocity of pre-equilibrum proton emission for such a mechanism. As seen in the figure, most pre-equilibrum particles are eliminated by the geometric and energetic thresholds of the detector arrays.

The events with complete charge detection were compared to simulations generated with the statistical code, GEMINI [16] and filtered by the detector acceptance. Two extreme excitation scenarios were considered: complete fusion in which the projectile and the target form a thermalized compound nucleus, and binary dissipative collisions in which a two-source system is produced, composed of a quasi-projectile and a quasi-target with different kinematic and energetic characteristics. The angular momentum input to the GEMINI code was determined from a comparison between experimental data and simulations made for different values of angular momentum. For the complete fusion scenario, we used the maximum angular momentum that can be sustained by the nucleus (25 $\hbar$), as determined from the prescription of Ref. [17]. For the dissipative binary collision scenario, the value of angular momentum was taken as proportional to the excitation energy of the nucleus, without exceeding the maximum sustainable angular momenta. The simulated disintegrations produced with GEMINI were transformed into the laboratory frame. The complete events were then passed through the experimental filter reproducing the geometry and energy thresholds of the multi-detector array. The filtering also took into account isotopic variations and

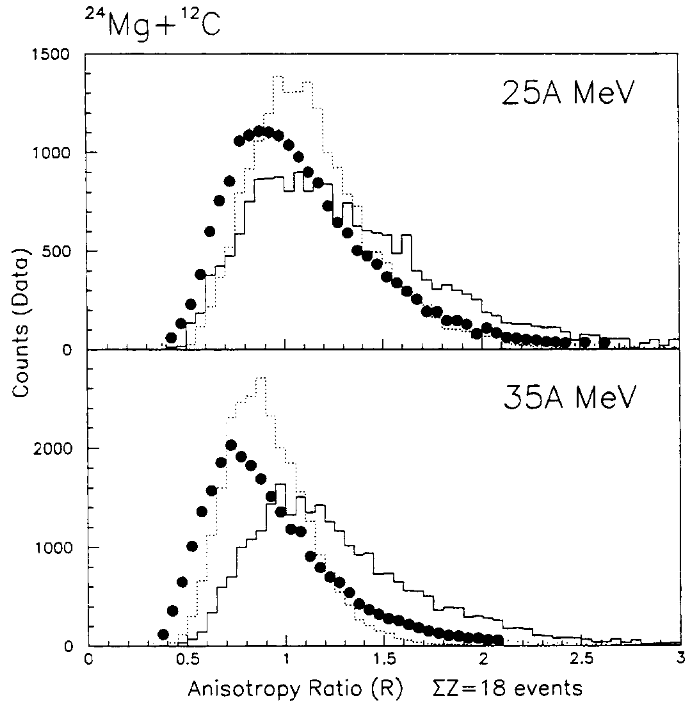

Fig. 3: Anisotropy ratio distributions, with R as defined in eq. (1), for completely detected experimental events (ΣZ=18) and the corresponding filtered simulations at 25A MeV (top) and 35A MeV (bottom). Filled circles represent experimental data, full lines complete fusion simulations with GEMINI, and dashed lines dissipative-binary collision simulations with TORINO and GEMINI.

the position uncertainty due to the large solid angle of each detector. Only the filtered events with ΣZ=18 were retained for the comparison. The charged-particle multiplicities of the filtered events in both excitation scenarios were consistent with, but slightly higher than, the experimental data.

The elongation of the distribution of a collision's reaction products in velocity space is an important observable for distinguishing binary and fusion-like reaction mechanisms. Quantitatively, a global variable can be constructed from a comparison of the longitudinal and transverse momentum components of the event's constituent particles [18]. This anisotropy ratio, R , is defined as

$$R = \frac{2}{\pi}\frac{\sum_{i=1}^{M} |P_{iCM\perp}|}{\sum_{i=1}^{M} |P_{iCM\parallel}|}, \tag{1}$$

where $\frac{2}{\pi}$ is a geometric normalisation constant, M is the charged-particle multiplicity, and $P_{iCM\parallel}$ and $P_{iCM\perp}$ are momenta of the i^{th} particle in the CM frame, perpendicular and parallel to the beam axis. Fig. 3 shows anisotropy ratio distributions compared to simulations, for both beam energies. The dissipative binary simulations show a better fit to the data at both beam energies. Fig. 4 shows the anisotropy distribution as a function of charged-particle multiplicity for experimental events with ΣZ=15, 16 or 17, and for both experimental and simulated events with ΣZ=18 at both beam energies. The effect of the experimental acceptance on the anisotropy ratio distributions may be deduced from the horizontal lines representing the R distributions for primary or "unfiltered" simulations, averaged over all multiplicities. It is important to note that the R distributions are skewed about their centroids and that the widths of

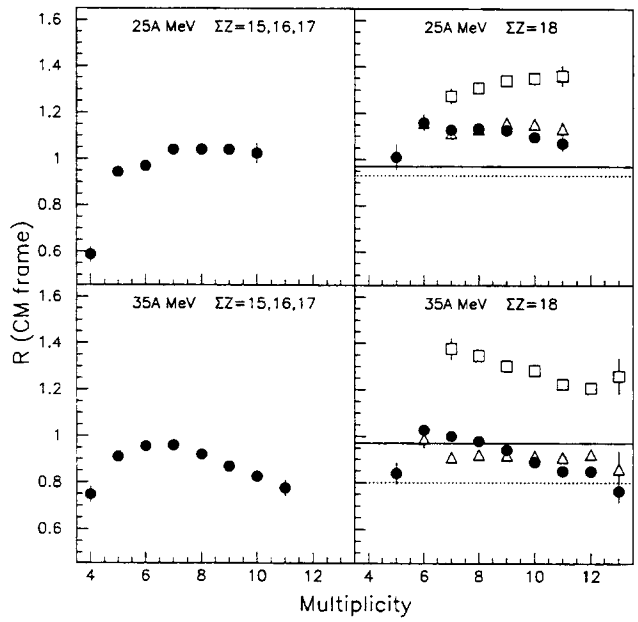

Fig. 4: Centroids of the anisotropy ratios versus multiplicity for incompletely detected events (ΣZ=15,16,17) at 25*A* MeV (top left) and 35*A* MeV (bottom left). Completely detected experimental events (ΣZ=18) and the corresponding filtered simulations are shown for 25*A* MeV (top right) and 35*A* MeV (bottom right). Filled circles represent experimental data, open squares complete fusion simulations with GEMINI, and open triangles dissipative-binary collision simulations with TORINO and GEMINI. Error bars are the root-mean square of *R*, divided by the square-root of the number of counts. The horizontal lines represent *R* centroids for unfiltered simulations for complete fusion (full lines) and dissipative binary collisions (dashed lines).

the distributions vary. Consequently, the experimental acceptance may highlight the difference between two distributions having similar "unfiltered" centroids, as is the case in the 25*A* MeV simulations.

Simulated complete fusion events were obtained for the disintegration of a ^{36}Ar compound nucleus, recoiling at center-of-mass velocity. The excitation energy was set to the maximum available in the CM reference frame, *i.e.* 200 MeV for events from the 25*A* MeV reaction and 280 MeV for the 35*A* MeV reaction. In the simulation of dissipative binary collisions, the excitation energy and scattering angle of both the quasi-projectile and the quasi-target were provided by the semi-classical coupled-channels code, TORINO [19]. The code requires the input of an impact parameter, from which it deduces the subsequent course of the reaction. For systems as light and energetic as ours, this should not necessarily be taken as the geometric trajectory of the entrance channel, but rather as a relative scale for the violence of the interaction. The impact parameter that best reproduces the anisotropy ratios at 25*A* MeV is 5.1 fm, which gives excitations of 95 and 81 MeV and velocities of 74% and 57% of the projectile velocity for the projectile-like and target-like sources, respectively. At 35*A* MeV, the best agreement is obtained for 4.1 fm, giving the corresponding excitation energies of 145 and 98 MeV, and velocities of 76% and 51% of the projectile velocity. At both energies, the anisotropies, measured as a function of multiplicity, are found to be similar for the incompletely detected (ΣZ=15, 16, or 17) and completely detected

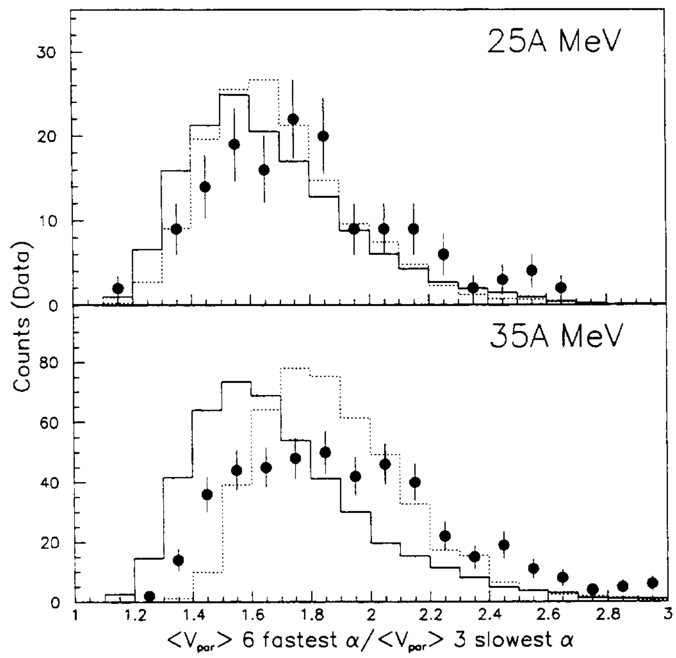

Fig. 5: Ratio between the average parallel velocities of the six fastest alpha-particles and the three slowest alpha-particles in the $^{24}Mg+^{12}C \rightarrow 9$ He channel at 25A MeV (top) and 35A MeV (bottom). Experimental events are shown as filled circles. The full line represents filtered complete fusion events simulated with SOS and the dotted line indicates the filtered TORINO-SOS simulation of dissipative binary collisions. Error bars show the square root of the number of counts.

($\Sigma Z=18$) events. For the complete events, at both energies, the anisotropy ratios lie close to the values predicted by the dissipative binary simulation at all multiplicities. Of particular interest is the dependence of R upon beam energy. Clearly, at 35A MeV, the anisotropy values deviate more from the fusion predictions than at 25A MeV. This suggests that, as the beam energy increases, the two sources become increasingly separated in velocity space.

The $\Sigma Z=18$, 9-He exit channel of this reaction was studied in somewhat greater detail, permitting an analysis with less isotopic ambiguity. We were able to treat this as a 9-α channel. A similar competition between fusion and binary mechanisms was observed. Here the simulations were done with the sequential part of the statistical code SOS [20], modified by its author to produce exit channels containing only α-particles. The initial conditions for the complete fusion simulation were the same as those for the GEMINI calculations, but with no angular momentum consideration. As before, TORINO was used to produce the conditions for the binary simulations, with a small range of impact parameters, rather than a single value, for each energy. In order to get the best possible fit to the experimental data, impact parameters from 5.0 to 6.0 fm and from 4.0 to 5.0 fm were selected for the 25A MeV and 35A MeV reactions, respectively. Fig. 5 shows the ratio between the average parallel velocity of the 6 fastest alpha-particles and the average velocity of the 3 slowest alpha-particles. This choice of variable is based on the products expected from the decay of a $^{24}Mg^*$ quasi-projectile and a $^{12}C^*$ quasi-target. Both simulated distributions resemble the data at 25A MeV, though the data may be somewhat closer to the dissipative binary collision case. At $35A$ MeV, the binary character of the 9-α channel is evident.

4. Conclusions

In conclusion, the reconstructed CM velocity distributions have confirmed the validity of the energy calibration and demonstrated the value of total charge detection in the determination of source properties. We have compared the anisotropies and source-velocity ratios observed experimentally for complete events with the results of simulations filtered by our detector response. The comparisons indicate that as the energy of the collision increases, binary mechanisms may compete successfully with simple compound nucleus formation.

The fact that the binary simulations, which assume two very different sources in size, velocity and excitation energy, give a better fit to part of the data may be explained by various reaction mechanisms. However, to properly assess these mechanisms, detailed data, such as those presented here, should be compared with a model that treats the dynamics of source formation as well as pre-equilibrium emission and the subsequent statistical decay.

We thank R.J. Charity, J.A. Lopez and J.-P. Wieleczko for the use of their statistical codes. This work was supported in part by the Natural Sciences and Engineering Research Council of Canada.

5. References

[1] D.H.E. Gross, Rep. Prog. Phys. 53(1990)605, and references therein.
[2] L.G. Moretto and G.J. Wozniak, Ann. Rev. Nucl. Phys. 1993, and refs. therein.
[3] H. Morgenstern et al., Phys. Rev. Lett. 52(1984)1104.
[4] D.R. Bowman et al., Phys. Lett. B189(1987)282.
[5] Y. Blumenfeld et al., Phys. Rev. Lett. 66(1991)576.
[6] K. Hanold et al., Phys. Rev. C48(1993)723.
[7] B. Lott et al., Phys. Rev. Lett. 68(1992)3141.
[8] J.F. Lecolley et al., Phys. Lett. B325(1994)317.
[9] C.A. Pruneau et al., Nucl. Instr. and Meth. in Phys. Res. A297(1990)404.
[10] J. Pouliot et al., Nucl. Instr. and Meth. in Phys. Res. A270(1988)69.
[11] Y. Larochelle et al., Nucl. Instr. and Meth. in Phys. Res. A348(1994)167.
[12] S. Kox et al., Nucl. Phys. A420(1984)162.
[13] C.A. Ogilvie et al., Phys. Rev. C40(1989)654.
[14] A. Malki et al., Z. Phys. A - Atoms and Nuclei 339(1991)283.
[15] J.P. Wieleczko, E. Plagnol and P. Ecomard, Proc. of the 2nd TAPS Workshop, Editors Diaz, Martinez and Shutz, Guardemar 1993, World Scientific, p.145.
[16] R.J. Charity et al., Nucl. Phys. A483(1988)371.
[17] R. Schmidt and H.O. Lutz, Phys. Rev. A45(1992)7981.
[18] H. Ströbele, Phys. Rev. C27(1983)1349.
[19] C.H. Dasso and G. Pollarolo, Comp. Phys. Comm. 50(1988)341.
[20] J.A. Lopez and J. Randrup, Comp. Phys. Comm. 70(1990)92.